

Nanosecond flash photolysis study of carbon monoxide binding to the β chain of hemoglobin Zürich [$\beta 63(\text{E7})\text{His} \rightarrow \text{Arg}$]

(heme protein/ligand binding/protein dynamics/conformational relaxation/sequential-barrier model)

DANA D. DLOTT*, HANS FRAUENFELDER*, PETER LANGER*, HEINRICH RODER*, AND ERNESTO E. DI IORIO†

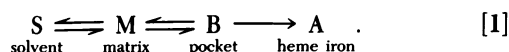
*Department of Physics and School of Chemical Sciences, University of Illinois at Urbana-Champaign, Urbana, IL 61801; and †Laboratorium für Biochemie, Eidgenössische Technische Hochschule, 8092 Zürich, Switzerland

Contributed by Hans Frauenfelder, June 20, 1983

ABSTRACT Binding of carbon monoxide to β chains of hemoglobin Zürich has been studied by flash photolysis over the time range of nanoseconds to seconds at temperatures from 20 to 300 K. From 20 to 200 K a single rebinding process (process I) is seen, characterized by a distribution of barrier heights with a peak enthalpy of 2.3 kJ/mol. Above 200 K some ligands escape from the pocket into the matrix, and above 260 K recombination from the solvent sets in. Process I is visible up to 300 K, but above 200 K its rate remains essentially constant at about $4 \times 10^9 \text{ s}^{-1}$. Above about 250 K, process I is exponential in time, indicating rapid conformational relaxation. The results are discussed within the framework of a sequential model for ligand binding.

Binding and dissociation of small ligands, such as O_2 and CO , to monomeric heme proteins is one of the simplest biological reactions. Early studies near physiological temperatures explained binding as a one-step process in which the ligand, coming from the solvent, overcomes a barrier of unspecified origin to bind at the heme iron (1). The work of Austin *et al.* (2), using flash photolysis and covering wide ranges in temperature (2–320 K) and time (microseconds to thousands of seconds), led to a model in which a ligand must overcome a series of sequential barriers (2). The model implies that proteins exist in a large number of structurally related conformational substates (2, 3), and that the innermost barrier, at the heme, is still present at physiological temperatures. Moreover, the experiments suggest that even at physiological temperatures the heme barrier, rather than diffusion (4, 5), controls binding (2, 6, 7). Because understanding one simple biological process in full detail may lead to deeper insight into more complex phenomena, it is crucial to prove or disprove the central features of the sequential-barrier model.

In the sequential-barrier model (2, 7, 8), a ligand coming from the solvent (S) migrates through the protein matrix (M) to the heme pocket (B) and overcomes a final barrier at the heme to bind covalently to the heme iron (state A):



In a photodissociation experiment, the system starts out in state A. The laser pulse breaks the Fe—CO bond and the system moves rapidly from A to B (9). In the heme pocket the ligand is essentially free (10, 11). Further evolution of the system depends on temperature. Below about 160 K, each protein rebinds its ligand from the pocket (process I). Process I is not exponential in time but approximately follows a power law. We explain this observation by postulating that there is a distri-

bution of barrier heights, $g(H_{\text{BA}})$, over the ensemble of molecules. The fraction of proteins that have not rebound a ligand at the time t after photodissociation is given by

$$N(t) = \int_0^\infty dH_{\text{BA}} g(H_{\text{BA}}) \exp[-k_{\text{BA}}(H_{\text{BA}}, T)t]. \quad [2]$$

Above about 40 K, the rate coefficient k_{BA} for the step $\text{B} \rightarrow \text{A}$ is given by an Arrhenius relation,

$$k_{\text{BA}}(H_{\text{BA}}, T) = A_{\text{BA}}(T/T_0)^\xi \exp(-H_{\text{BA}}/RT), \quad [3]$$

where T_0 is an arbitrary reference temperature and ξ is a free parameter. Without loss of generality, we take $T_0 = 100 \text{ K}$. Below 40 K, tunneling through the barrier becomes dominant and Eq. 3 is no longer valid (12, 13). Earlier, Eqs. 2 and 3 with $\xi = 0$ were used to fit the observed rebinding functions $N(t)$ in a wide variety of heme proteins (2, 7, 14).

In Mb, at temperatures above about 160 K, some ligands move into the protein matrix, migrate in the matrix, return to the pocket, and bind. Above about 200 K, some ligands move from the matrix into the solvent. We denote with $N_{\text{out}}(T)$ the fraction of systems initially in state B that move to state S. All ligands in the solvent then compete for the vacant binding site; the rate of the solvent process consequently is proportional to the ligand concentration. The solvent process is exponential in time, with a pseudo-first-order rate coefficient λ_{on} . The nonexponential time dependence at low and the exponential time dependence at high temperatures can be explained in terms of conformational substates and relaxation (2, 3): Each protein can exist in a large number of structurally similar substates that interconvert with an average relaxation rate λ_r . At low temperatures, λ_r is small compared with rebinding rates and each protein is frozen into a particular substate with a corresponding barrier height H_{BA} . At high temperatures, λ_r becomes large compared with λ_{on} and rebinding is exponential in time; λ_{on} can then be written as (7)

$$\lambda_{\text{on}}(T) = \bar{k}_{\text{BA}}(T) P_{\text{B}}(T) N_{\text{out}}(T) \quad [4]$$

$$\bar{k}_{\text{BA}}(T) = \int dH_{\text{BA}} g(H_{\text{BA}}) k_{\text{BA}}(H_{\text{BA}}, T) \quad [5]$$

where $\bar{k}_{\text{BA}}(T)$ is an average rate coefficient for the step $\text{B} \rightarrow \text{A}$ and $P_{\text{B}}(T)$ is the probability of finding state B in the limit $k_{\text{BA}} \rightarrow 0$.

Eq. 5 assumes that the low temperature distribution $g(H_{\text{BA}})$ is also relevant at high temperatures at which it relaxes to its mean value \bar{H}_{BA} . This point will be discussed below.

The central assumptions underlying Eq. 4 are (i) process I still operates at high temperatures, (ii) binding is sequential as

The publication costs of this article were defrayed in part by page charge payment. This article must therefore be hereby marked "advertisement" in accordance with 18 U.S.C. §1734 solely to indicate this fact.

shown in Eq. 1, (iii) extrapolation of the rate coefficient \bar{k}_{BA} with Eq. 5 is valid, and (iv) the temperature is high enough so that the relaxation rate (λ_r) is fast compared with the binding rate (λ_{on}).

All experimental data available are consistent with the four assumptions, but proofs are incomplete. A direct verification of, for instance, assumption i should consist in following process I from low temperatures, where only I is seen, to about 300 K. The difficulty of such an experiment with most heme proteins can be realized by considering the scheme Eq. 1. In a first approximation, N_I , the fractional intensity of direct rebinding, can be written as $N_I = (1 + k_{BM}/k_{BA})^{-1}$, where k_{BM} is the effective rate coefficient for moving from B to M. If $k_{BM}/k_{BA} \gg 1$, as is the case for instance in Mb-CO at 300 K, N_I becomes very small and I is consequently difficult to observe. Assuming that k_{BM} is similar in different heme proteins, the best chance to follow process I up to high temperature exists in a protein that has a small BA barrier so that k_{BA} at 300 K is large. Fortunately such a protein exists: In the isolated β chain of hemoglobin Zürich, β^{ZH} (15, 16), the distal histidine is replaced by arginine and the average barrier between B and A is only about 2 kJ/mol, one-fifth of that in myoglobin (7) or half of that in normal β chains. The small barrier is one among several features distinguishing the mutant protein from the normal one (7, 15, 16), which demonstrates the importance of the distal residue in controlling ligand binding. In the present paper, we show that flash photolysis experiments with β^{ZH} indeed permit observation of process I up to 300 K.

MATERIALS AND METHODS

The β chains (β^{ZH}) of hemoglobin Zürich with regenerated SH groups were separated as described elsewhere (16). The samples were stored in the CO-bound form in liquid nitrogen. Samples for flash photolysis were prepared by diluting the concentrated stock solution to a final concentration of ≈ 1 mM in 75% glycerol (vol/vol)/0.1 M potassium phosphate, buffering the solution at pH 7. The solvent was initially saturated with 1 bar (1 bar = 100 kPa) CO. Dithionite was added to remove residual O_2 . In the 0.8-mm sample cells, the optical density at our monitor wavelength (442 nm) was between 0.5 and 0.6. It is likely that the β^{ZH} chains form tetramers as is known for β^A (17).

The flash photolysis apparatus used to study the kinetics of CO recombination at times longer than 50 ns has been described (7). The absorbance change induced by the 30-ns laser pulse at 530 nm was monitored at 436 nm. We extended the time resolution down to about 1 ns by using as the photolyzing source a frequency-doubled Nd/YAG laser (532 nm) that pumps a dye laser (Rhodamine 6G dye), producing a 15-ps 5- μ J pulse at 570 nm with a maximum repetition rate of 500 Hz (18). The sample was placed in a closed-cycle helium refrigerator. The exciting beam was focused down to ≈ 150 μ m on the sample, photolyzing $\approx 50\%$ of the molecules. The continuous 442-nm light of a helium/cadmium laser (Liconix 4210) was passed through the photolyzed sample volume with an angle of a few degrees between the two laser beams. After passing through a monochromator, the 442-nm beam was monitored with a photomultiplier tube (1P28A) with a pulse-response time of 1.5 ns FWHM. For most experiments, the flash-induced transmission changes were recorded with a sampling oscilloscope (Tektronix 7S12 with S2 sampling head). The sampling rate was 500 Hz, synchronized with the exciting laser pulses. The sweep time was 2 s, resulting in 1,000 samples per sweep. The time scale covered by one sweep was varied between 20 and 200 ns. To get sufficient time for baseline recording before the exciting pulse,

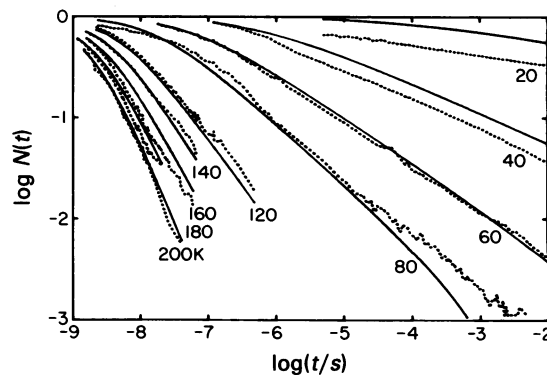


FIG. 1. Rebinding of CO to β^{ZH} in 75% glycerol/water. \cdots , Experimental data, measured at 20–200 K; —, fit to the data as described in the text. The resulting enthalpy distribution is shown in Fig. 3.

the detector output signal was delayed. Typically, 600–800 sweeps were averaged in a 12-bit signal averager and plotted on an x-y recorder. The raw data were transferred to a CYBER-170 computer (Control Data, Minneapolis, MN) by tracing the curves on a digitizer board. A limited number of traces (40–120 K) were recorded with a Tektronix 7912 transient digitizer system equipped with a minicomputer. The flash repetition rate in this case was 2–5 Hz so that complete recombination between flashes was ensured. The main source of noise was intensity fluctuations in the He/Cd laser.

For a single sweep of the sampling scope, the signal-to-noise ratio was ≈ 2 . After signal averaging 600–800 sweeps, a signal-to-noise ratio of ≈ 50 was obtained. The zero point of the time scale was determined by recording the detector response to the exciting laser pulses with the monitor beam blocked. These traces also revealed some artifacts due to cable reflections and small residual laser pulses after the main pulse. Artifacts in the signal traces correlated to those in the laser pulse response were removed during data analysis. In the experiments with the picosecond laser, we normalized each trace individually by extrapolating on a semilogarithmic plot to $t = 0$ and matching the traces at different time scales. For the data obtained with the nanosecond laser, the traces at all temperatures were normalized with the constant determined at 40 K. The two data sets matched well in the overlap region (≈ 100 ns). The measured absorbance change was independent of the monitor light intensity and did not change when the flash repetition rate of the exciting laser was reduced. Consequently the two laser beams

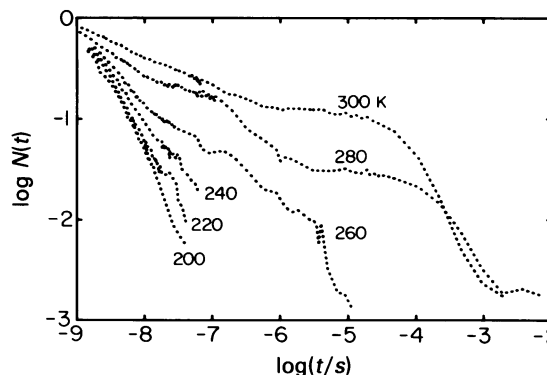


FIG. 2. Rebinding of CO to β^{ZH} in 75% glycerol/water at 200–300 K. The solvent process is seen at 280 and 300 K. The data from about 0.1 μ s to 10 ms were obtained with the flash-photolysis equipment described previously (7).

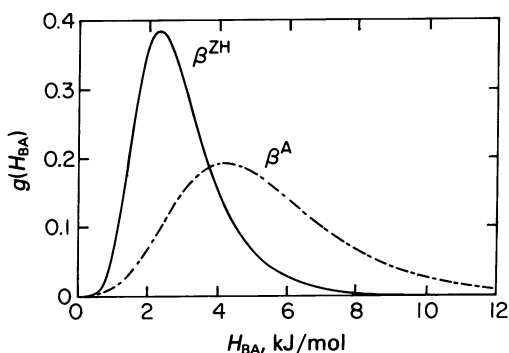


FIG. 3. Activation enthalpy distribution $g(H)$ for β^{ZH} and β^{A} . The curves were calculated with the analytical $g(H)$ from ref. 14, using the parameters that produced the best agreement with the experimental data shown in Fig. 1. The parameters for β^{ZH} (β^{A}) are $H_p = 2.3$ kJ/mol (4.2 kJ/mol), $A_{\text{BA}} = 1.5 \times 10^9$ s $^{-1}$ (1.1×10^9 s $^{-1}$), and $\xi = 1$ (0).

did not cause significant sample heating and the monitor light induced no additional photolysis.

RESULTS

With only two optically distinct states involved, CO-bound and ligand-free [the amplitudes of other states are expected to be small (19)], the observed absorbance change is proportional to $N(t)$, the fraction of molecules that have not rebound a ligand at time t . The kinetics of binding of CO to β^{ZH} is shown as plots of the logarithm of $N(t)$ versus the logarithm of t in Figs. 1 and 2. Fig. 1 shows a single nonexponential rebinding process below 200 K. We associate it with process I, the transition from the pocket state B to the bound state A (Eq. 1). The solid curves are calculated from Eqs. 2 and 3 by using an analytical form with three free parameters (the peak enthalpy H_p and two shape parameters) for $g(H_{\text{BA}})$ (14). H_p , A_{BA} , and ξ were varied to find the best simultaneous fit to the data from 60 to 200 K. The fits in Fig. 1 and the distribution function in Fig. 3 were achieved with $H_p = 2.3 \pm 0.3$ kJ/mol, $A_{\text{BA}} = 1.5 \times 10^9$ s $^{-1}$, and $\xi = 1$. Similar fits were obtained by varying ξ between 0.8 and 1.2 and adjusting A_{BA} within a factor of 3. It was not possible, however, to reproduce the data with a temperature-independent preexponential factor ($\xi = 0$). Data below 60 K were not considered, since their temperature dependence may be affected by tunneling. Also shown in Fig. 3 is $g(H_{\text{BA}})$ for normal β chains (14), which peaks at the significantly higher enthalpy $H_p = 4.2$ kJ/mol.

Above 200 K, the shape and the temperature dependence of $N(t)$ change as shown in Fig. 2. Between 210 and 260 K a second (slower) process (M) appears. Above 260 K, a third approximately exponential and even slower process (S) with strongly

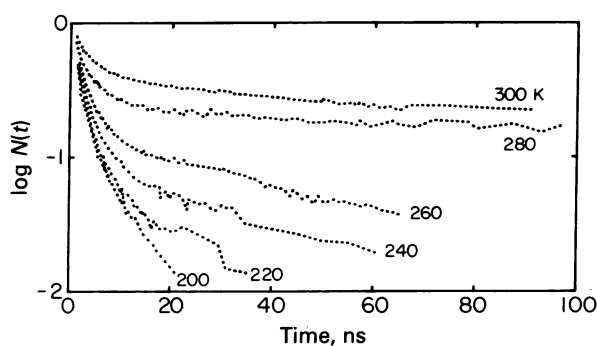


FIG. 4. Expanded semilogarithmic plot of the data in Fig. 2. The fast process I can be clearly distinguished from the slower process M.

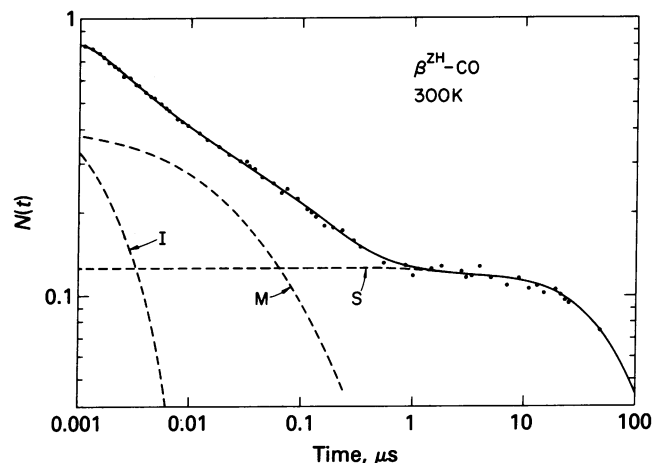


FIG. 5. Decomposition of the trace recorded at 300 K into processes S, M, and I. While S and I are exponential in time, M clearly is not.

temperature-dependent amplitude develops. The rate of process S is proportional to CO concentration and we consequently identify it as the second-order recombination from the solvent (state S in Eq. 1). At 300 K the rate of solvent recombination, λ_{on} , at 1 bar (1 bar = 100 kPa) CO is 1.2×10^4 s $^{-1}$, and the amplitude, which corresponds to the fraction N_{out} of ligands escaping into the solvent, is 0.12. Normal β chains in the same solvent have $\lambda_{\text{on}} = 2.2 \times 10^3$ s $^{-1}$ and $N_{\text{out}} = 0.3$ (13). Fig. 4 is an expanded semilogarithmic plot of the high-temperature kinetics of β^{ZH} -CO, showing the two internal processes I and M.

We separate the processes present above 200 K by subtracting the slower processes S and M from $N(t)$, as shown in Fig. 5 for the 300 K data. The subtraction of S is straightforward in Fig. 2. It is, however, difficult to recognize the presence of two processes, I and M, in the log-log plot Fig. 2 that covers the entire range of $N(t)$ and t . The separation of process M is therefore carried out in an expanded plot as for instance in Fig. 4. Fig. 5 and corresponding data at other temperatures between 200 and 300 K provide the following information on the processes I, M, and S: I decreases and M and S increase with increasing temperature, as is shown in Fig. 6, which gives the

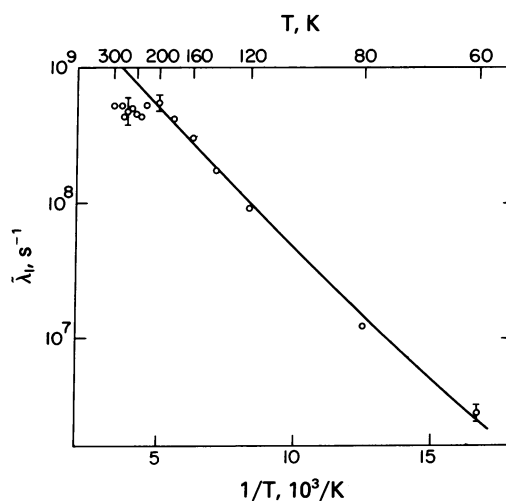


FIG. 6. Plot of $\bar{\lambda}_1$ versus $10^3/T$. $\bar{\lambda}_1$ is the rate corresponding to a decrease in amplitude of process I to $1/e$ of its initial value. The solid line was constructed from the theoretical fits in Fig. 1; the slight curvature reflects the temperature-dependent preexponential term in Eq. 3.

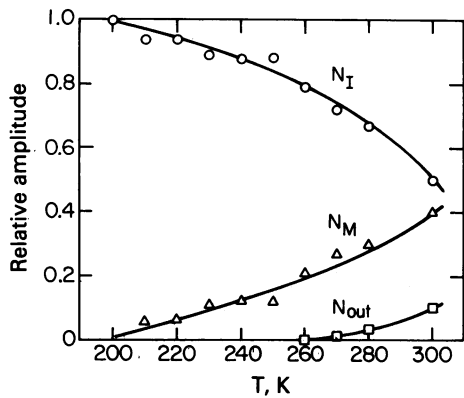


FIG. 7. Relative amplitudes of process I (N_I), matrix process (N_M), and solvent process (N_{out}) at 200–300 K.

relative amplitudes N_I , N_M , and N_{out} as a function of temperature. Process I is clearly observable up to 300 K. At 200 K, I is given by a power law; at 300 K, it has become exponential. The change from power law to exponential time dependence occurs at about 250 K. The rate of process I becomes essentially temperature independent above 200 K, deviating from what is expected from the extrapolation of the low-temperature data with Eqs. 2, 3, and 5. The discrepancy is illustrated in Fig. 7, in which an effective rate λ_I determined from the time of decay to $1/e$ of the initial amplitude is plotted versus $10^3/T$. The deviation is outside the uncertainty introduced by the subtraction of the slower processes. While processes I and S are exponential in time at 300 K, process M is unambiguously not, as is shown in Fig. 5. The nonexponential time dependence of M is even more apparent at temperatures between 240 and 280 K. At these temperatures, $N_M(t)$ follows a power law [$N_M(t) \propto t^{-n}$] with $n \approx 0.5$ over nearly 2 orders of magnitude in time.

DISCUSSION

The results shown in Figs. 2–7 test some of the assumptions underlying the sequential-barrier model. Four central assumptions were stated in the *Introduction* and we discuss them here in the same order.

(i) **Process I at High Temperatures.** Figs. 1, 2, and 5 show that direct rebinding after flash photolysis, process I, can be observed from 20 to 300 K. This fact implies that the innermost barrier at the heme is present at all temperatures.

(ii) **Sequential Barriers.** In our model, Eq. 1, the barrier at the heme is also the final step in binding at physiological temperatures. In other models (4, 5), the low- and the high-temperature reactions are assumed to occur in parallel. The present data are consistent with both sequential and parallel barriers. Earlier, it was found, however, that the pH dependence of the binding of CO to Mb and the β^A chain at high temperatures is given by the pH dependence of process I at low temperatures (7). Barring an unlikely coincidence, this relation implies sequential steps.

(iii) **Extrapolation of the Low-Temperature Data.** In our earlier work, Eqs. 3 and 5 were used to extrapolate the low-temperature data to 300 K. In the present work, we determine k_{BA} directly. Fig. 6 shows that the quantitative agreement between the calculated and the measured k_{BA} does not extend beyond 200 K for β^{ZH} . At 300 K, the observed rate falls short of the extrapolated one by about a factor of 3. One explanation for such a deviation from Arrhenius behavior has been suggested by Agmon and Hopfield (20): The protein structure immedi-

ately after photodissociation is known to differ from the deoxy structure. At temperatures below 200 K, the protein will remain in this structure. Above 200 K, the protein may relax into the deoxy conformation, thus modifying the B \rightarrow A transition. If k_{BA} is smaller in the deoxy structure, the binding rate can level off in the temperature range at which the conformational equilibrium shifts from the ligated to the deoxy structure. Our analysis of a simple model involving a transition between two B states has shown that such a model indeed can fit the observed temperature dependence. The difference between the CO-bound and the deoxy structure is larger in β^{ZH} than for instance in Mb. X-ray crystallography (21, 22) shows movement of the distal arginine sidechain (arginine E7) and rearrangement of several groups in the vicinity of the heme. Although the x-ray studies were carried out on Hb^{ZH} tetramers, it is likely that the β^{ZH} tetramers will also undergo major changes. An alternative explanation for the behavior of process I is suggested by another structural feature found by x-ray diffraction of β^{ZH} (21, 22): The distal arginine E7 interacts with the propionate of the heme, leaving the pocket wide open whereas in normal β chains access to the active site is blocked by the distal histidine. Since the gap is wide enough to allow access of sulfanilamides to the iron (21); it is likely that the solvent also enters the pocket. The binding kinetics could therefore be affected by changes in the solvent properties (in glycerol/water a liquid-glass transition is known to occur near 200 K). Preliminary flash photolysis data of β^{ZH} in solvents of different viscosities indicate that process I indeed depends on the solvent while in myoglobin, where the entrance to the pocket is blocked, this effect is much smaller.

(iv) **Conformational Relaxation.** Fig. 5 shows that process I is exponential in time at 300 K. The transition from nonexponential to exponential time dependence occurs around 250 K, but the limited accuracy of the data and the uncertainty introduced by the subtraction of the slower processes makes it difficult to determine the transition temperature accurately. The data imply a relaxation rate $\lambda_r \geq 10^8 \text{ s}^{-1}$ at 300 K, consistent with values from Mössbauer and Rayleigh scattering experiments on Mb (23–25). Since λ_{on} is of the order of 10^4 s^{-1} (Fig. 2), $\lambda_r \gg \lambda_{on}$ and assumption iv is satisfied.

Our data yield other information.

(v) **The Arrhenius Relation.** Because of the small H_{BA} in β^{ZH} , the temperature dependence of the preexponential factor A_{BA} can be studied. A satisfactory fit of the data up to 200 K (Figs. 1 and 6) was obtained by using a preexponential factor of the form $A_{BA}(T/T_0)^\xi$ with ξ in the range of 0.8 to 1.2 and assuming a temperature-independent activation enthalpy distribution, $g(H_{BA})$. The data cannot be fit with $\xi = 0$. We cannot, however, exclude the possibility that $g(H_{BA})$ changes with temperature.

(vi) **Process M.** Fig. 5 shows the presence of a process that we call M; M is independent of the ligand concentration in the solvent and nonexponential in time. The time τ^M at which the amplitude is reduced to $1/e$ of its initial value is about 50 ns at 300 K. This process has been observed in Mb (2) and the separated Hb chains (14) at temperatures up to about 280 K and called "processes II and III." At around 300 K, a fast geminate binding has been seen by a number of groups (26–30). Lindqvist *et al.* (29), in particular, noticed that this geminate rebinding was not exponential in time. The characteristic time τ^M observed in β^A (29) and Mb (30) is also of the order of 100 ns. We interpret process M as rebinding from the protein matrix. In contrast, Agmon and Hopfield (20) interpret a similar process in their calculation as being due to rebinding from the pocket in the relaxed protein. Since the rebinding process shown in their work is exponential in time and the experimentally observed process M is close to a power law, we favor the inter-

pretation that process M is due to migration of the ligand through the protein matrix and the solvation layer.

With this paper, we wish to acknowledge the work of Eraldo Antonini, who was a pioneer in this field. We thank S. F. Bowne, W. Doster, W. A. Eaton, J. J. Hopfield, M. F. Perutz, L. Reinisch, D. L. Rousseau, E. Shyamsunder, K. H. Winterhalter, and R. D. Young for helpful discussions and critical comments. This work was supported in part by Grant PHS GM 18051 from the Department of Health and Human Services, by Grant PCM 79-05072 from the National Science Foundation, and by a fellowship from the North Atlantic Treaty Organization Science Council through the Deutscher Akademischer Austauschdienst to P.L.

1. Antonini, E. & Brunori, M. (1971) *Hemoglobin and Myoglobin in Their Reactions with Ligands* (North-Holland, Amsterdam).
2. Austin, R. H., Beeson, K. W., Eisenstein, L., Frauenfelder, H. & Gunsalus, I. C. (1975) *Biochemistry* **14**, 5355-5373.
3. Frauenfelder, H., Petsko, G. A. & Tsernoglou, D. (1979) *Nature (London)* **280**, 558-563.
4. Hasinoff, B. B. (1981) *J. Phys. Chem.* **85**, 526-531.
5. Hasinoff, B. B. & Chishti, S. B. (1983) *Biochemistry* **22**, 58-61.
6. Beece, D., Eisenstein, L., Frauenfelder, H., Good, D., Marden, M. C., Reinisch, L., Reynolds, A. H., Sorensen, L. B. & Yue, K. T. (1980) *Biochemistry* **19**, 5147-5157.
7. Doster, W., Beece, D., Bowne, S. F., DiIorio, E. E., Eisenstein, L., Frauenfelder, H., Reinisch, L., Shyamsunder, E., Winterhalter, K. H. & Yue, K. T. (1982) *Biochemistry* **21**, 4831-4839.
8. Eisenstein, L. & Frauenfelder, H. (1982) in *Biological Events Probed by Ultrafast Laser Spectroscopy*, ed. Alfano, R. R. (Academic, New York), pp. 321-337.
9. Martin, J. L., Migus, A., Poyart, C., Lecarpentier, Y., Astier, R. & Antonetti, A. (1983) *Proc. Natl. Acad. Sci. USA* **80**, 173-177.
10. Alben, J. O., Beece, D., Bowne, S. F., Doster, W., Eisenstein, L., Frauenfelder, H., Good, D., McDonald, J. D., Marden, M. C., Moh, P. P., Reinisch, L., Reynolds, A. H., Shyamsunder, E. & Yue, K. T. (1982) *Proc. Natl. Acad. Sci. USA* **79**, 3744-3748.
11. Ondrias, M. R., Rousseau, D. L. & Simon, S. R. (1983) *J. Biol. Chem.* **258**, 5638-5642.
12. Alberding, N., Austin, R. H., Beeson, K. W., Chan, S. S., Eisenstein, L., Frauenfelder, H. & Nordlund, T. M. (1976) *Science* **192**, 1002-1004.
13. Alben, J. O., Beece, D., Bowne, S. F., Eisenstein, L., Frauenfelder, H., Good, D., Marden, M. C., Moh, P. P., Reinisch, L., Reynolds, A. H. & Yue, K. T. (1980) *Phys. Rev. Lett.* **44**, 1157-1160.
14. Alberding, N., Chan, S. S., Eisenstein, L., Frauenfelder, H., Good, D., Gunsalus, I. C., Nordlund, T. M., Perutz, M. F., Reynolds, A. H. & Sorensen, L. B. (1978) *Biochemistry* **17**, 43-51.
15. Winterhalter, K. H., Anderson, N. M., Amiconi, G., Antonini, E. & Brunori, M. (1969) *Eur. J. Biochem.* **11**, 435-440.
16. Giacometti, G. M., Brunori, M., Antonini, E., DiIorio, E. E. & Winterhalter, K. H. (1980) *J. Biol. Chem.* **255**, 6160-6165.
17. Valdes, R. & Ackers, G. K. (1977) *J. Biol. Chem.* **252**, 74-81.
18. Dlott, D. D., Schosser, C. L. & Chronister, E. L. (1982) *Chem. Phys. Lett.* **90**, 386-390.
19. Hofrichter, J., Sommer, J. H., Henry, E. R. & Eaton, W. A. (1983) *Proc. Natl. Acad. Sci. USA* **80**, 2235-2239.
20. Agmon, N. & Hopfield, J. J. (1983) *J. Chem. Phys.* **78**, 6947-6959.
21. Tucker, P. W., Phillips, S. E. V., Perutz, M. F., Houtchens, R. & Caughey, W. S. (1978) *Proc. Natl. Acad. Sci. USA* **75**, 1076-1080.
22. Phillips, S. E. V., Halle, D. & Perutz, M. F. (1981) *J. Mol. Biol.* **150**, 137-141.
23. Keller, H. & Debrunner, P. G. (1980) *Phys. Rev. Lett.* **45**, 68-71.
24. Parak, F., Frolov, E. N., Mössbauer, R. L. & Goldanskii, V. I. (1981) *J. Mol. Biol.* **145**, 825-833.
25. Krupnyanski, Yu. F., Parak, F., Goldanskii, V. I., Mössbauer, R. L., Gaubman, E. E., Englemann, H. & Suzdalev, I. P. (1981) *Z. Naturforsch. Teil C* **37**, 57-62.
26. Alpert, B., El Mohsni, S., Lindqvist, L. & Tfibel, F. (1979) *Chem. Phys. Lett.* **64**, 11-16.
27. Dudell, D. A., Morris, R. J. & Richards, J. T. (1979) *J. Chem. Soc. Chem. Commun.*, 75-76.
28. Dudell, D. A., Morris, R. J., Muttucumar, N. J. & Richards, J. T. (1980) *Photochem. Photobiol.* **31**, 479-484.
29. Lindqvist, L., El Mohsni, S., Tfibel, F., Alpert, B. & Andre, J. C. (1981) *Chem. Phys. Lett.* **79**, 525-528.
30. Henry, E. R., Sommer, J. H., Hofrichter, J. & Eaton, W. A. (1983) *J. Mol. Biol.* **166**, 443-451.